Comparative study on the NDT testing at elevated temperature

Supriya Purumani, Assistant Professor, Department of Civil Engineering, Geethanjali College of Engineering and Technology (Autonomous), Hyderabad

ABSTRACT: *Computer Tomography (CT) is a digital x-ray imaging method in which a narrow beam of x-rays is sighted at an object and quickly revolved around the target, generating signals to produce cross-sectional images or "slices" of the body. These slices are called tomographic images and contain more detailed information than conventional x-rays. After several successive tomographic photographs are collected, they can be digitally "stacked" together to form a three-dimensional image. The present project focuses on predicting the extent of thermal damage on hydrated Portland Cements (PC) using Computer Tomography (CT). The hydrated specimens of Portland Cement (PC) were subjected to temperatures ranging from 27 °C − 800 °C, for an interval of every 100 °C was analyzed. The 3d image of Specimen with pores is generated using a CT scan. Furthermore, samples of a material can be analyzed under different loading conditions or only progressive compression loading to observe the changing of the internal structure of the material, which provide an insight into the fracture and failure mechanism of concrete.*

Spectroscopy is the interaction between matter and electromagnetic radiation, which is useful in the determination and characterization of various chemical compositions existing in the material. Present paper, focuses on predicting the extent of thermal damage on hydrated Portland Cements (PC), using Fourier Transform Infrared Spectroscopy (FTIR). The hydrated specimens of Portland Pozzolana Cement (PPC) and Ordinary Portland Cement (OPC), were subjected to temperatures ranging from 27 °C − 800 °C, for an interval of every 100 °C was analyzed. Variation in the absorbance peaks obtained from FTIR, is correlated with the Thermal analysis (TA). At temperatures beyond 400 °C, reduction in the absorbance values at wavenumbers of 3430 – 3440 cm−1 of Ettringite phase for PPC and OPC specimens was observed. However, in OPC specimens, an increase in the absorbance values of Portlandite phase at wavenumbers ranging from 3640 to 3645 cm−1 was observed. The phase changes taking place in the PC specimens observed using FTIR, are in good agreement with the mass loss and heat flow plots obtained from TA. Therefore, it can be concluded that FTIR analysis is suitable test method in predicting the thermal damage of concrete specimen.

Key words: Computer Tomography, x-ray, slices, tomographic images, stacked, Ordinary Portland Cement, Fourier Transform Infrared Spectroscopy.

1. INTRODUCTION

Concrete has superior thermal behavior under fire, with respect to steel, as it has less thermal conductivity. Even though concrete has better thermal behavior under fire, the damage done to human life and materials is beyond measure. Several studies on the thermal behavior of concrete have indicated, that physicochemical changes are not observed at temperatures less than 80 ℃. An escape of free and physically bound water causes a drying shrinkage at ~ 100 ℃, and initiation of hydrothermal reactions at ~105 ℃. The decomposition of Calcium Silicate Hydrate (CSH) is a continuous process at temperatures beyond 120 ℃, micro cracks are developed with the increasing porosity, at temperatures exceeding 300 ℃ results in a reduction of compressive strength. At 400 ℃ – 600 ℃ dissociation of Portlandite (Ca (OH)2) takes place and cracks are visible on the surface of the hydrated cement paste, while decarbonization of Calcite (CaCO3) i.e., CaO + CO2 at temperatures beyond 700 ℃. However, the escaping of chemically bound water takes place at 800 ℃, at this point the concrete disintegrates [4].

Thermal behaviors of concrete are often an interesting and challenging area of research. Many new techniques are still in progress to determine the severity of the damage caused to structural members, for predicting their durability and serviceability. Methods such as X-Ray Diffraction (XRD), Scanning Electron Microscopy (SEM), Thermal Analysis (TA), Computer Tomography (CT) Spectroscopy analysis I.e., Infrared Spectroscopy (IR) and Raman Spectroscopy (RS) tools are commonly used. The major advantages of spectroscopy analysis are, the smaller quantity of sample required for investigation. OPC specimens are subjected to 27 ℃ - 1000 ℃ of temperatures and were analyzed using XRD, TG/DTA. The extent of the damage at the surface and core of the specimens varied for the Portlandite phase, which isn't the case for the Calcite [1]. At 300 ℃, Portlandite intensity increased due to the recrystallization of amorphous hardened cement paste [2]. Hydrated paste at extreme temperature leads to irreversible decomposition reaction, which leads to changes in mineralogical composition [3]. Lucia Alaron-Ruiz analyzed thermal treated hydrated cement specimens using environmental SEM and TGA. A reduction in weight and expansion of capillary pores in hydrated samples was observed at temperatures beyond 400 ℃ [5]. PC with varying specific surface area (SSA) and compressive strength, for the hydration periods of 1-6 years analyzed using TA and XRD. XRD analysis indicated a continuous reduction in Portlandite peak up to 450 ℃. Limestone and Fly ash (FA) specimens subjected to 250 ℃ - 850 ℃ were analyzed using DSC, XRD. An increase in compressive

strength at 250 °C was due to the formation of additional hydration of un-hydrous grains, due to the deposition of CSH [6].

Table 1.1: Chemical formulas of cement phases present in PC

Cement phases	Chemical composition	Common name
Calcium Aluminate Sulphate	$3Ca_6Al_2(SO_4)_3(OH)_{12}.26(H_2O)$	Ettringite
Calcium Aluminoferrite Hydrate	$Ca_2(Al, Fe)_2O_5$	-
Calcium Carbonate	$CaCO_3$	Calcite
Calcium Hydroxide	$Ca(OH)_2$	Portlandite
Calcium Monosulfate	$CaO\ Al_2O_3\ CaSO_4\ 12(H_2O)$	AFm
Calcium Monosulphoaluminate	$6CaO\ Al_2O_3\ Fe_2O_3\ 12(H_2O)$	-
Calcium Sulphate Hydrate	$CaSO_42H_2O$	Gypsum
Calcium–Silicate–Hydrate	$Ca_5Si_6O_{16}(OH)_2.4H_2O$	CSH
Di-aluminium Tri-oxide	Al_2O_3	Aluminate
Di-Calcium Silicate	$2CaO.SiO_2$	Belite
Hydro-Garnet	$Ca_3Al_2(OH)_{12}$	-
Lizardite	$Mg_3Si_2O_5\ (OH)_2$	-
Magnesium Carbonate	$MgCo_3$	-
Magnesium Oxide	MgO	Periclase
Tetra-Calcium Aluminate Ferrite	$4CaO.Al_2O_3Fe_2O_3$	Ferrite
Tri-Calcium Aluminate	$3CaO.Al_2O_3$	Celite
Tri-Calcium Silicate	$3CaO.SiO_2$	Alite

Silica fume (SF) was replaced in PC, and hydrated specimens were exposed to elevated temperatures and analyzed using TA, XRD. A good correlation exists in TA, but not for XRD due to the poor crystallinity of the CH phase [7]. A significant absorbance peak of Alite, Belite, and Portlandite phases were formed in the region of 500 cm-1 & 900 cm-1 [8]. The CSH phases of Tobermorite-11Å, -14 30 Å and Jennite have a similar structure which is analyzed using IR. An increase in the pores volume and percentage porosity with the increasing temperature is leading to the crack propagation. The specimen tested using computer tomography shown a good result of visualization of internal pores.

A shift towards the lower wavenumber results in the stretching of bonds existing in between the chemical oxides, due to the reduction of polymerization [9]. FTIR can be used as a quantifying tool, to predict the quantities of certain phases existing in the cement sample [10]. FTIR and Thermal analysis were extensively used, for estimating the changes taking place, in the various phases, present in the hydrated PC, at various temperatures. However, no literature was observed in correlating the physical damage taking place in hydrated PPC and OPC-53 specimens with respect to TG/DTA and FTIR analysis. As the primary difference between the PPC and OPC-53 specimens, are the varying concentrations of silicon dioxide and SSA. Hence, the variations taking place in between the chemical oxides need to be understood to determine the extent of damage in PC under thermal load and how far the test methods under consideration can differentiate between the GoC is determined.

X-ray computer tomography (CT) is fast becoming an accepted tool within the materials science community for the acquisition of 3D images. Our review considers first the image acquisition process, including the use of iterative reconstruction strategies suited to specific segmentation tasks and emerging methods that provide more insight (e.g., fast and high-resolution imaging, crystallite (grain) imaging) than conventional attenuation-based tomography. Methods and shortcomings of CT are examined for the quantification of 3D volumetric data to extract key topological parameters such as phase fractions, phase contiguity, and damage levels as well as density variations. As a non-destructive technique, CT is an ideal means of following structural development over time via time lapse sequences of 3D images (sometimes called 3D movies or 4D imaging). This includes information needed to optimise manufacturing processes, for example sintering or solidification, or to highlight the proclivity of specific degradation processes under service conditions, such as inter granular corrosion or fatigue crack growth. Besides the repeated application of static 3D image quantification to track such changes, digital volume correlation (DVC) and particle tracking (PT) methods are enabling the mapping of deformation in 3D over time. Finally, the use of CT images is considered as the starting point for numerical modelling based on realistic microstructures, for example to predict flow through porous materials, the crystalline deformation of polycrystalline aggregates or the mechanical properties of composite materials.

2. OBJECTIVES OF THE PROJECT

1: Evaluate the behaviour of the cements at the elevated temperatures

2: The limitations of the present available non-destructive testing's

3: Application of the Computer tomography (CT) and Fourier transform infrared spectroscopy (FTIR).

4: Reduction of the strength with the increasing temperature Objective 5: Effect of the increasing porosity on the compressive strength.

3. LITERATURE REVIEW

Hung et al. 2003, when cement-based materials are exposed to the high temperatures induced by fire, which can rapidly cause temperatures of over 1000 °C, the changes in pore structure and density prevail

Deville et al. have studied the solidification of ice crystals in a ceramic aqueous slurry in a process called freeze casting to produce lamellar porous ceramics with tomograms acquired in 1 second and a voxel size in the reconstruction of 1-7 µm.

K. H. Khor 2016, it is found that the tensile strength decreases as the void fraction increases, and the relative strength of cement paste and interfaces dominates the micro cracking behaviour, which in turn affects macrocracking and load-carrying capacity.

Chung et al, 2019, the extent of the damage at the surface and core of the specimens varied for the Portlandite phase, which isn't the case for the Calcite.

4. EXPERIMENTAL INVESTIGATION

Specimen Preparation

Cubes of size 50 × 50 × 50 mm3 are cast for the two GoC [11] i.e., PPC and OPC-53, tests are carried at a 100 °C interval from Ambient temperature (27 °C) to 800 °C, i.e. A total of 27 cubes each, for PPC and OPC-53. While an average normal consistency value of 0.33 was adopted, as the water-cement (W/C) ratio for all the specimens. The cast specimens were dried for 24 hrs demoulded, and left in curing for a period of 28 days. On the day of testing, the specimens are taken out of curing tank, and dried to air. A set of three specimens each, are placed in the muffle furnace for thermal loading, at their respective temperatures as shown Figure 3.1. Once the specimens have reached their desired temperatures, they are left in the furnace to get back to the ambient temperature. The specimens obtained from the furnace at the respective temperatures are tested under compressive testing machine, for determining the compressive strength of the specimens.

Once the samples compressive strengths are determined for the respective temperatures, the cores obtained from the test specimens are collected, for conducting spectroscopy and TA. These collected samples are further pulverized in a planetary ball mill to obtain uniform fineness. For which 30 grams of sample is placed in wiles at a ratio of 1:10, sample to weight ratio and particles are dispersed using Toluene. The input parameters for the planetary ball mill are 300 rpm, this procedure is carried out for 30mns out of which for every 5mins of rotations 5mins is the resting time. Then the sample is collected and dried at room temperatures to obtain dry powder for further studies. The pulverized samples obtained from ball at their respective temperatures, are further analyzed under FTIR and Thermal analysis. A specimen for FTIR is made using 250 mg of Potassium Bromide (KBr) and 3 mg of cement powder, and compacted into a pellet.

Similarly, the sample of Concrete (150 mm x 150 mm x 150 mm), Mortar (70.1 mm x 70.1 mm x 70.1 mm) and Cement (50 mm x 50 mm x 50 mm) were casted at room temperature with 0.4 normal consistency. These Cube were first heated to different temperature as show in the figure 3.1, once the cubes reach the desired temperatures, they were sent to testing in computer tomography to analyses the porosity of the different cube heated to the different temperature. The topographical images of the cubes are considered and later analyzed in Avizo for the 3D and volumetric analysis.

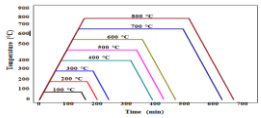

Fig. 4.1. Temperature profile of hydrated PC specimens

4.1 Evaluation methods

4.1.1. X-Ray Fluorescence (XRF)

To predict the chemical oxide composition of PPC and OPC-53, the tests are conducted on Bruker S4 Pioneer.

4.1.2. Thermo Gravimetric Analysis (TGA)

TGA of the samples of PPC and OPC-53 was conducted with the help of NETZSCH STA 2500 at a heating rate of 10 °C/min in argon atmosphere with an initial temperature of 27 °C and with temperatures going up to 800 °C to determine their response (i.e., the percentage of mass loss with respect to the original weight).

4.1.3. Differential Temperature Analysis (DTA)

DTA of PPC and OPC-53 cast samples were conducted using NETZSCH STA 2500 at a heating rate of 10 °C/min in an argon atmosphere with an initial temperature between 27 °C going all the way to 800 °C. This analysis helps in estimating the endothermic or exothermic behaviour of the sample by recording the difference in the temperature between the sample and reference material (i.e., Alumina).

4.1.4. Fourier Transform Infrared Spectroscopy (FTIR)

Infrared spectroscopy was conducted using Perkin-Elmer® Model 100 FTIR over a range of 400 to 4000 cm-1 with an accuracy of ± 2% with a transmission mode.

4.1.5 Computer tomography (CT)

Tested on128 Slice GE Optima CT660 Computed Tomography System for all the specimens at the Radar Diagnostic Centre Warangal.

5. RESULT AND DISCUSSION

5.1 XRF analysis

The XRF results of the un-hydrated samples for the PPC and OPC-53 GoC are as shown in Table 2. According to the British code the concentrations of major and minor oxides are: SiO2 is 21-22%, Fe2O3 is 0.5-5%, SO3 ≤ 1.5%, two GoC have exceeded the recommended values, while Al2O3 should be in the ranges of 3-8%. The PPC has exceeded the concentration limits as per the British code [12], while the CaO was less than the required i.e., 60-67% for PPC. The XRF analysis indicate, OPC-53 concentrations of CaO are greater, while the SiO2 concentrations are higher for PPC.

Table 5.1 Chemical oxide concentrations of PPC and OPC-53

Chemical Composition	PPC (%)	OPC-53 (%)
CaO	37.6	66.6
SiO_2	34.72	16.77
AL_2O_3	11.8	3.1
Fe_2O_3	6.99	5.78
SO_3	4.00	5.1
K_2O	1.29	0.51
TiO_2	1.01	0.3
MgO	0.58	1.01
Na_2O	0.21	0.07
MnO	0.15	0.11
P_2O_5	0.39	0.16
SrO	0.08	0.09

5.2 Thermal analysis (TA)

As mentioned above the SiO2 concentrations are higher in PPC, due to the inclusion of FA, which is a by-product of Coal, used as a fuel in the thermal power plant. As coal is subjected to temperatures closer to 1500 - 2000 °C, the obtained FA has better thermal behaviour. To understand the variations in the mass loss and heat flow, of PPC and OPC-53 GoC, TA studies are conducted. Under TA, three fundamental tests exist i.e., TGA, DTA, and DSC. However, for the current studies TGA and DTA tests are performed, and the results obtained from these tests are as below:

5.3 Thermogravimetric analysis (TGA)

TGA estimates the absolute amount of change and rate of change in the weight of the sample, which is a function of time or temperature in a controlled environment. Using TGA, properties such as thermal stability, atmosphere effects at different conditions, oxidative stability, moisture, and volatile content, can be determined. The plots obtained from the TGA analysis of the PPC and OPC-53 specimens are shown in Figure 2(a). The plots have shown three critical regions of mass loss, At the first region, located between 100 and 200 ℃, due to dehydration reactions of several hydrates such as un-hydrated water, CSH, Carbo Aluminates, Ettringite etc.[13]. The Mass loss taking place in PPC and OPC-53 samples are almost linear i.e., at 27 ℃ - 150 ℃ is 8.3 and 7.7%. The second major mass loss, observed at 400 – 500 ℃, corresponds to the dihydroxylation of Portlandite, which is one of the identifiable major products during hydration [13]. The respective mass loss for PPC and OPC-53 at these temperature regions are 1.7 and 3.4%, the mass loss taking place in OPC-53 sample is twice the mass taking place in PPC. Mass loss taking place at 600 - 750 °C as observed in Figure 2(a), is due to the decarbonization of Calcite into CaO and CO2, observed in both PPC and OPC-53 samples. Arguably, reaction taking place due to decarbonation of Calcite is relatively higher in PPC, which resulted in higher mass loss. However, the mass loss at these temperatures for PPC and OPC-53 samples is 4.50 and 1.45%. The mass loss taking place in the PPC sample is three times to that of OPC-53. Due to the excess mass loss in PPC specimens, the hairlines are visible on the surface of the PPC specimens Figure 5(C). It is observed that the overall mass loss taking place in PPC samples (22%) is greater than the OPC-53 (19.50%).

5.4 Differential thermal analysis (DTA)

The plots obtained from the DTA, for the PPC and OPC-53 specimens, using an aluminium crucible, at the temperature ranges3 27 - 800 °C is shown Figure 2(b). The PPC samples have shown four regions of interest, and the first endothermic peak is at 63 ℃, and the second being at 99 ℃, such peaks are due to the evaporation of un-

hydrated and bound water from the samples. Water present in the hydrated cement paste, can be completely evaporated from the samples at 120°C [14]. Alarcon-ruiz et al. observed two endothermic peaks at the temperatures of 110 °C – 170 °C, due to the decomposition of Gypsum, Ettringite, and loss of water in the Carbo-Aluminates, however, such peaks are not observed for the two GoC. A continuous loss of mass takes place from 171 °C -300 °C due to the decomposition of CSH, which releases the bound water present in the gel. This phenomenon can be observed from the TGA plots and such a mass loss can have an effect on the heat flow, as observed from the DTA plots. The third endothermic peak is observed in the PPC sample at 428 °C, is due to the de-hydroxylation of Portlandite from the hydrated cement paste. The fourth endothermic peak is observed in PPC the sample at 702 °C, is formed due to the de-carbonation of Calcium Carbonate and this followed by a mass loss observed in the TGA plot of PPC. Similar to the PPC analysis, the OPC-53 has shown two ROI, which is at 87°C, and 432 °C respectively. One can infer From Figure 2(b), that the heat flow taking place in PPC is relatively lower, with respect to OPC-53. Such a superior resistance to heat flow in is due to the temperatures, in which the FA is produced, and is used as a partial replacement in PPC.

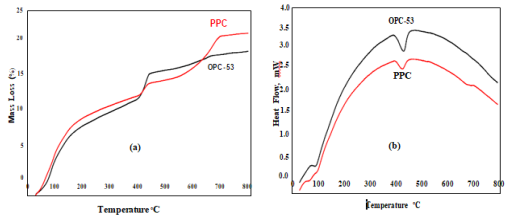

Fig.5.1. (a) TGA and (b) DTA analysis of PPC and OPC-53

5.5 FTIR analysis

FTIR spectroscopic is a useful, Non-destructive, easy technique, which requires a few milligrams of a material understudy for determining the chemical composition present in it, by determining the existing chemical bonds present in a material. Using FTIR analysis, it is possible to detect crystalline and amorphous phases that are frequently developed in PC, at different in-situ conditions. The molecule's energy is dependent on electron's motion in the molecule, constituent atoms vibrations, and rotation of the molecule as a whole. The excitation vibrations caused by the molecules in the IR region causes the adsorption bands. FTIR predicts the chemical compounds in the material by studying the vibrational properties of amorphous as well as crystalline samples, as it comes in contact with IR. As the molecules absorb IR, which further converts into energy that causes molecular vibrations. Absorbance takes place, only when the radiant energy produced due to the contact of IR matches to that of a specific molecular vibration. Every chemical group present in the molecules has a unique frequency to absorb the radiation. The vibrations of atoms in the molecules are categorized as stretching and bending. While some bonds can stretch in-phase or out of phase i.e. symmetrical stretching or asymmetric stretching [14]. The plots obtained from the FTIR analysis of PPC and OPC-53 samples, temperatures ranging from 100 °C – 800 °C with a 100 °C interval are shown in Figure 3(a), (b). For ease in understanding and analysis, the transmission plots are converted into absorbance.

The wavenumber region of 400 - 1000 cm-1 corresponds to bending vibrations, 1001 – 1500 cm-1 corresponds to single bond stretches, 1501 – 2000 cm-1 corresponds to double bond stretch, 2001 – 2500 cm-1 corresponds to triple bond stretch, and 2501 – 4s000 cm-1 corresponds to Z-H single bond stretch such as O-H, N-H, and C-H bonds [15]. The Absorbance peak at Wavenumber 457 cm-1 is observed for PPC at 100 °C and there is a shift towards the higher wavenumber for both PPC and OPC-53 samples up to 400 °C. At the temperatures of 500 °C, such peak was not observed. This absorbance peak can play a significant importance, to predict the temperatures of the PC.

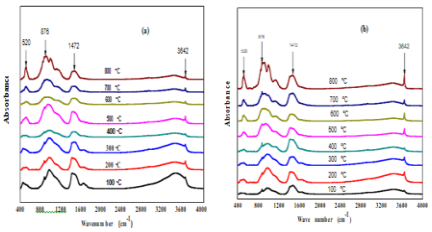

Fig. 5.2 FTIR graphs of (a) PPC (b) OPC-53

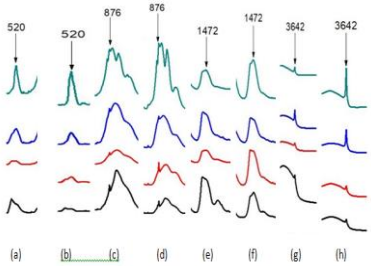

Fig. 5.3 Peak at 100 °C, 400 °C, 500 °C, 800 °C of (a, c, e, g) PPC, (b, d, f, h) OPC-53.

A strong absorbance peak was developed at wavenumber 517-520 cm-1 of C3A or C4AF phases, at temperatures above 400 °C was observed for PPC but not for OPC- 53 at all temperatures. One of the primary reasons is due to the concentrations of CaO in OPC-53 is 66.6%, while in PPC is 37.6%, due to the variations in these concentrations

an increase or decrease in Absorbance bands can be noted, and shown in Figure 4(a) and (b). The Absorbance peaks at the Wavenumber region of 870-1000 cm-1 is an indication of C2S polymorphs i.e. β-C2S [9]. Two peaks are observed in the region of 870 – 1000 cm-1 at 100 °C; 874, 971 cm-1 which represent the β-C2S are observed. As the temperatures increase to 800 °C four peaks are observed i.e., of 846, 875, 915 and 996 cm-1. A significant Absorbance peak was developed as the PPC and OPC-53 were subjected temperatures beyond 700 °C, at wavenumber of 915 and 997 cm-1. A decrease in bond length, is represented by a shift in Absorbance values towards lower wavenumber. The Calcite Absorbance peak observed at 3450 cm-1 for PPC and 3434 cm-1for OPC-53 at 27 °C, shifted to lower wavenumber with the increase in temperature i.e., 3417 and 3420 cm-1. The increase in the Absorbance value of Wavenumber 3642 cm-1 as shown in Figure 4(g) and (h), is significant in the PPC and OPC-53 samples at temperatures beyond 500 °C. From the current experimental study, the Absorbance peak observed in OPC-53 sample is relatively higher with respect to PPC sample at wavenumber of 3642 cm-1. As the endothermic peak formed in the region of 400 - 500 °C, is due to the reduction of the Portlandite phase, can be related to an increase in the concentration of Calcium Oxides.

5.4 Compressive strength

The PPC and OPC-53 specimens (50 × 50 × 50 mm3) subjected to elevated temperatures in a muffle for the desired heating and cooling cycles shown in Figure 1. The failure pattern taking place on the surface of the PPC and OPC-53 at 400 °C, 500 °C, and 800 °C is as shown in Figures 5 & 6. The hydrated samples of PPC and OPC-53 samples below 400 °C, did not show any signs of failure on the external surface. The PPC samples at temperatures exceeding 400 °C are still intact and are able to withstand external loads, while the OPC-53 samples failed due to thermal loads. The disintegration of the hydrated cement specimens from Figure 6(b) & (c) of OPC-53 specimens, is clearly evident at temperatures of 500 °C and above. While the PPC specimens are still intact as shown in Figure 5(b) & (c) and are able to withstand the external loads. The Compressive strengths of the PPC and OPC-53 samples at elevated temperatures are shown in Figure 7. The loss in compressive strength of PPC samples is 5.61%, 22%, 37% and 61% at temperatures of 100 °C, 400 °C, 500 °C and 800 °C, while for OPC-53 it is 10%, and 49% at 100 °C and 400 °C respectively. TA studies indicate a mass loss taking place due to the loss of hydrated water present in the hydrated PC samples, contributed to the loss in compression strength at the temperature ranges of 27 °C – 400 °C. The drop in the mass loss as shown in Figure 2(a), did not lead to any physical changes, which are observed on the surface of the PPC and OPC-53 specimens Figure 5(a) and 6(a) at 400 °C. Once the specimen's temperatures are in the ranges of 400 °C – 500 °C, the TGA graph from Figure 2(a), shows a sudden increase in mass loss, due to the disintegration of Portlandite. The dissociation of the Portlandite leads to noticeable physical changes, that are visible on the surface of the PPC and OPC-53 specimens as shown in Figure 5(b) & 6(b). Even though the dissociation of the Portlandite has caused a lot of cracks in OPC-53 at 500 °C, which lead to the disintegration of specimen Figure 6(b). The PPC specimen behavior is completely different, as observed in Figure 5(b), i.e., specimens were able to withstand the external compressive loads. This behavior of PPC specimens is due to superior thermal resistance to heat flow with respect to OPC-53. As the DTA analysis Figure 2(b), has shown that the heat flow taking place in OPC-53 is greater with respect to PPC.

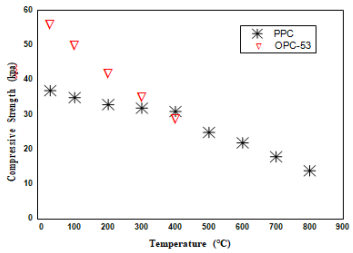

Fig 5.4 Compressive strength of PPC and OPC-53 specimens at various temperatures.

5.5 Computer tomography (CT)

The graph Plotted between Compressive strength and Temperature for Cement, Mortar, Cement clearly showing the reduction of the strength with the increasing porosity. At first, we can observe the evolution of temperature changes in the specimen. The specimens were cast with Portland cement, at 100°C, an increase in porosity of the material detect and caused by the evaporation of adsorbed water and a decrease in material density. At 500°C concrete loses its stability significantly. At 700°C, cracks inside pores have increased because of the decomposition of the C-S-H gel. At 1000°C thermal expansion of cracks and extensive cracking is observed.

In fig 5.5 the temperature increment is directly resulting in the increment of the Porosity value of the sample. Comparatively the cement has the high porosity at the initial temperature but at the elevated temperature mortar is resulting with high porosity.

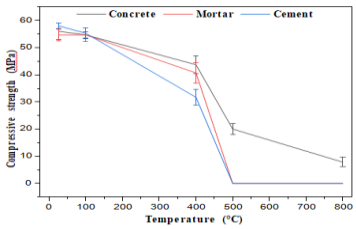

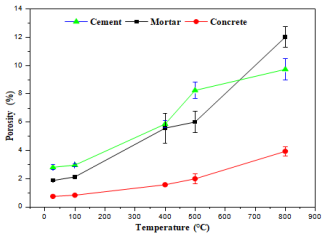

Fig 5.5 Compressive strength Vs Temperature **Fig 5.6 Porosity Vs Temperature**

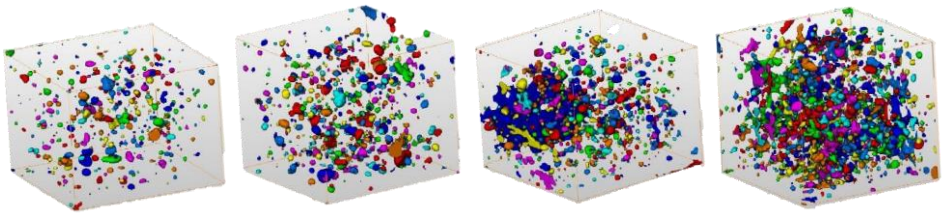

a)100 °C *b)400 °* *c)500 °C* *d)800 °C*

5.7 Porosity Images of Concrete

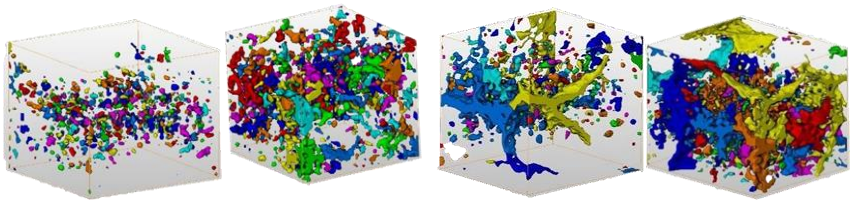

a)100 °C *b)400 °C* *c)500 °C* *d)800 °C*

5.8 Porosity Images of Mortar

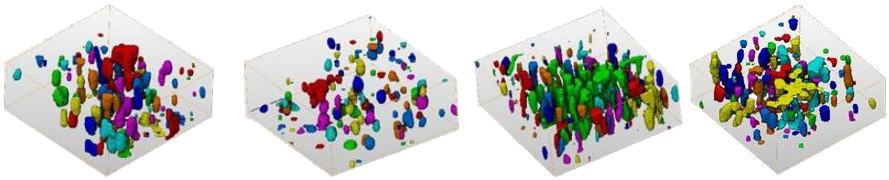

a)100 °C b)400 °C c)500 °C d)800 °C

5.9 Porosity Images of Cement

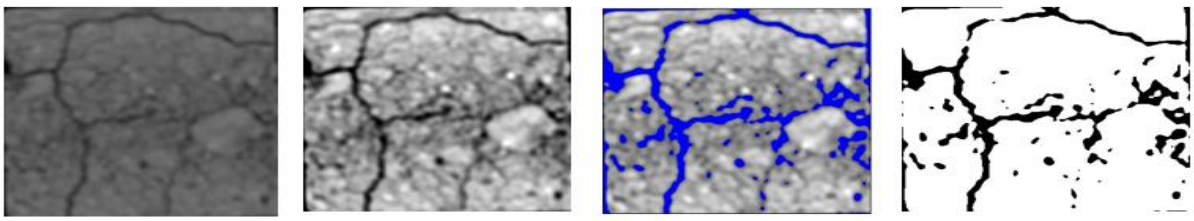

5.10 Thresholding of the Samples

6. CONCLUSION:

The experimental investigation carried in the current research article is to understand which GoC i.e., PPC and OPC-53, has a better thermal behaviour under thermal loads ranging from 27 °C – 800 °C. The physical changes taking place in the OPC-53 specimens were found to be very high with respect to PPC. To understand this phenomenon,

further investigations are conducted using XRF, TGA, DTA, CT and FTIR. From the present study, the following are the conclusion:

- The PPC specimens have shown superior thermal behaviour with respect to OPC-53 specimens at elevated temperatures even at temperatures of 800 °C. This is one of the special attributes that PPC posses with respect to other features, such as gradual development in strength, durability, higher specific surface area, etc.
- The PPC and OPC-53 specimens behaved differently under the same thermal loading conditions. Hence the usage of PPC is advisable and also economical. XRF studies indicate PPC has a higher concentration of SiO2 due to the inclusion of FA, while the CaO concentrations are higher for OPC-53.
- Even though the mass loss taking place in PPC and OPC-53 specimens are almost similar, observed from TGA. While, DTA indicated a higher heat flow rate, taking place in OPC-53 with respect to PPC specimens. Due to the superior heat flow taking place in OPC-53 specimens, under thermal loads, lead to the disintegration of hydrated OPC-53 samples.
- The porosity is directly affected with the increasing temperature and strength is decreased with the increasing porosity. CT scan has showed very good results with the regard of the strength and porosity.

REFERENCES

[1] S. K. Handoo, S. Agarwal, and S. K. Agarwal, "Physicochemical, mineralogical, and morphological characteristics of concrete exposed to elevated temperatures," Cem. Concr. Res., vol. 32, no. 7, pp. 1009–1018, 2002.
[2] I. Hager, "Behaviour of cement concrete at high temperature," Bull. Polish Acad. Sci. Tech. Sci., vol. 61, no. 1, pp. 145–154, 2013.
[3] A. Lucia, J. Hoyos, M. Perez, and J. L. Chicharro, "Heart rate and performance parameters in elite cyclists: A longitudinal study," Med. Sci. Sports Exerc., vol. 32, no. 10, pp. 1777–1782, 2000.
[4] W. Eike, "Research Collection," 2014.
[5] Q. Fu, N. Zhou, W. Huang, D. Wang, L. Zhang, and H. Li, "Preparation and characterization of a novel bioactive bone cement: Glass based nanoscale hydroxyapatite bone cement," J. Mater. Sci. Mater. Med., vol. 15, no. 12, pp. 1333–1338, 2004.
[6] A. S. Benosman et al., "Mineralogical Study of Polymer-Mortar Composites with PET Polymer by Means of Spectroscopic Analyses," Mater. Sci. Appl., vol. 03, no. 03, pp. 139–150, 2012.
[7] H. K. Choudhary et al., "Observation of phase transformations in cement during hydration," Constr. Build. Mater., vol. 101, pp. 122–129, 2015.
[8] S. N. Ghosh and A. K. Chatterjee, "Absorption and reflection infra-red spectra of major cement minerals, clinkers and cements," J. Mater. Sci., vol. 9, no. 10, pp. 1577–1584, 1974.
[9] F. Spectroscopy, "Structure of Calcium Silicate Hydrate (C-S-H): Near-, Mid-, and Far-Infrared Spectroscopy," vol. 48, pp. 742–748, 1999.
[10] M. Horgnies, J. J. Chen, and C. Bouillon, "Overview about the use of fourier transform infrared spectroscopy to study cementitious materials," WIT Trans. Eng. Sci., vol. 77, pp. 251–262, 2013.
[11] M. Kisan, S. Sangathan, J. Nehru, and S. G. Pitroda, "म ोा नक," 1967.
[12] A. Koksal, "British Standard A single copy of this British Standard is licensed to," no. May, 2003.
[13] L. P. Esteves, "On the hydration of water-entrained cement-silica systems: Combined SEM, XRD and thermal analysis in cement pastes," Thermochim. Acta, vol. 518, no. 1–2, pp. 27–35, 2011.
[14] M. Chollet and M. Horgnies, "Analyses of the surfaces of concrete by Raman and FT-IR spectroscopies: Comparative study of hardened samples after demoulding and after organic post-treatment," Surf. Interface Anal., vol. 43, no. 3, pp. 714– 725, 2011.
[15] T. Renuka Devi, K B, Durairaj, K S P; Chithambarathanu, "FTIR and FTR spectral analysis of some poly atomic molecules," Manonmaniam Sundaranar Univ., vol. chapter 2, 2009.
[16] T. M. Breunig, S. R. Stock, A. Guvenilir, J. C. Elliott, P. Anderson and G. R. Davis: 'Damage in aligned-fibre SiC/Al quantified using a laboratory X-ray tomographic microscope', Composites, 1993,
[17] P. J. Schilling, B. P. R. Karedla, A. K. Tatiparthi, M. A. Verges and P. D. Herrington: 'X-ray computed microtomography of internal damage in fiber reinforced polymer matrix composites', Compos. Sci. Technol., 2005.
[18] P. Cloetens, M. Pateyron-Salome, J. Y. Buffiere, G. Peix, J. Baruchel, F. Peyrin and M. Schlenker: 'Observation of microstructure and damage in materials by phase sensitive radiography and tomography', J. Appl. Phys., 1997.
[19] K. I. Ignatiev, W. K. Lee, K. Fezzaa, F. De Carlo and S. R. Stock: 'Phase contrast stereometry: Fatigue crack mapping in 3D', Developments in X-ray tomography IV, Proc. SPIE, 2004.
[20] K. H. Khor, J. Y. Buffiere, W. Ludwig, H. Toda, H. S. Ubhi, P. J. Gregson and I. Sinclair: 'In situ high resolution synchrotron X-ray tomography of fatigue crack closure micromechanisms', J. Phys. Condens. Matter, 2004.